Probing Cross-Bridge Angular Transitions Using Multiple Extrinsic Reporter Groups†

Katalin Ajtai, Andras Ringler, and Thomas P. Burghardt*
Department of Biochemistry and Molecular Biology, Mayo Foundation, Rochester, Minnesota 55905
Received May 29, 1991; Revised Manuscript Received August 7, 1991

ABSTRACT: ^{15}N- and ^{2}H-substituted maleimido-TEMPO spin label ([^{15}N,^{2}H]MTSL) and the fluorescent label 1,5-IAEDANS were used to specifically modify sulfhydryl 1 of myosin to study the orientation of myosin cross-bridges in skeletal muscle fibers. The electron paramagnetic resonance (EPR) spectrum from muscle fibers decorated with labeled myosin subfragment 1 ([^{15}N,^{2}H]MTSL-S1) or the fluorescence polarization spectrum from fibers directly labeled with 1,5-IAEDANS was measured from fibers in various physiological conditions. The EPR spectra from fibers with the fiber axis oriented at 90° to the Zeeman field show a clear spectral shift from the rigor spectrum when the myosin cross-bridge binds MgADP. This shift is attributable to a change in the torsion angle of the spin probe from cross-bridge rotation and is observable due mainly to the improved angular resolution of the substituted probe. The EPR data from [^{15}N,^{2}H]MTSL-S1 decorating fibers are combined with the fluorescence polarization data from the 1,5-IAEDANS-labeled fibers to map the global angular transition of the labeled cross-bridges due to nucleotide binding by an analytical method described in the accompanying paper [Burghardt, T. P., & Ajtai, K. (1992) *Biochemistry* (preceding paper in this issue)]. We find that the spin and fluorescent probes are quantitatively consistent in the finding that the actin-bound cross-bridge rotates through a large angle upon binding MgADP. We also find that, if the shape of the cross-bridge is described as an ellipsoid with two equivalent minor axes, then cross-bridge rotation takes place mainly about an axis parallel to the major axis of the ellipsoid. This type of rotation may imitate the rotational motion of cross-bridges during force generation.

The ability of extrinsic fluorescent or spin probes attached to protein elements of a biological assembly to detect protein rotation is related to the orientation of the probe relative to a reference frame fixed in the protein element. This is true because certain well-understood ambiguities in the techniques for measuring probe orientation limit the types of probe rotations that can be detected. Generally, it is essential to combine data from a family of different probes that are variously oriented within the protein fixed reference frame. Myosin cross-bridge orientation changes in skeletal muscle fibers demonstrate the advantage of using multiple probes since cross-bridge rotation is detected by a variety of fluorescent and spin probes, but the sensitivity of any single probe to a changing cross-bridge orientation varies greatly.

Maleimido-TEMPO spin label (MTSL) was shown to detect cross-bridge rotation when modifying sulfhydryl 1 (SH1) of myosin subfragment 1 (S1) decorating skeletal muscle fibers (Ajtai et al., 1989). The effect of cross-bridge rotation on the electron paramagnetic resonance (EPR) spectrum of MTSL-S1 was a subtle change in the spectral shape. We showed that another probe of myosin SH1, iodoacetamido-PROXYL spin label (IPSL), was more sensitive to cross-bridge rotation because it had a different orientation on the cross-bridge (Ajtai et al., 1990). We measured obvious spectral changes in the EPR spectrum from IPSL-S1 that indicated cross-bridge rotation.

In parallel experiments, the fluorescent probes 1,5-IAEDANS (15IA) and (iodoacetamido)tetramethylrhodamine (IATR) modifying SH1 also had differential sensitivities to cross-bridge rotation. The 15IA appeared to be less sensitive than IATR to cross-bridge rotation. We verified that this differential sensitivity was due to probe orientation on the cross-bridge by effectively rotating the transition dipoles (the vectors that define probe orientation when measured by fluorescence polarization) of the probes by excitation wavelength variation (Ajtai & Burghardt, 1987). In these experiments, we measured the fluorescence polarization excitation spectrum and showed that the sensitivity of the probes to cross-bridge rotation varied with wavelength in correlation with the rotation of the absorption dipole.

In this work, we introduce two innovations in the study of cross-bridge orientation changes. First, we use the novel spin probe the ^{15}N- and ^{2}H-substituted maleimido-TEMPO to modify SH1 on S1 ([^{15}N,^{2}H]MTSL-S1) and to detect cross-bridge orientation from decorated muscle fibers in rigor or in the presence of MgADP. We also report on the results from fluorescence polarization studies of 15IA-labeled fibers that employ excitation wavelength variation to improve sensitivity for detecting probe rotation. Second, we apply the analytical method introduced in the accompanying paper (Burghardt & Ajtai, 1992), to the problem of mapping cross-bridge rotational transitions under physiological state changes in muscle fibers. With this method, we combine data from [^{15}N,^{2}H]MTSL-S1 with previously measured data from IPSL-S1 decorating fibers and 15IA-labeled fibers to enhance the resolving power of the probes for detecting rotation. Our past and present studies with fluorescent and spin labels were performed on two different but comparable biochemical systems. The fluorescent probe is introduced directly into the myosin cross-bridges in glycerinated muscle fibers. This can be done without altering the ability of the muscle fiber to contract. This is not done with spin probes since fibers directly labeled with maleimido-TEMPO, then treated with potassium ferricyanide to remove the large nonspecific spin label popu-

† This work was supported by the National Science Foundation (DMB-8819755), the National Institutes of Health (RO1 AR 39288-O1A2), the American Heart Association (Grant-in-Aid 900644), and the Mayo Foundation. T.P.B. is an established investigator of the American Heart Association.
* To whom correspondence should be addressed.

0006-2960/92/0431-207$03.00/0

lation, lose Ca^{2+} sensitivity such that labeled fibers contract in the presence of MgATP but no Ca^{2+} (unpublished observation). Consequently, when using spin probes, we study cross-bridge orientation with decorated fibers, i.e., when specifically spin-labeled S1 is diffused into intact glycerinated fibers. This system is a model for the cross-bridge attached states of the contraction cycle.

The replacement of ^1H with ^2H near to the nitroxide group in spin labels decreases the spectral line width by reducing proton broadening and consequently increases the signal-to-noise ratio for the detection of the EPR signal by ~5-fold (Hwang et al., 1975; Beth et al., 1981). The narrowed line width also enhances the resolution of the spin probe angular distribution determined from the EPR spectrum (Burghardt & Thompson, 1985). Replacing ^{14}N with the stable isotope ^{15}N in the nitroxide group couples the electron spin, via the hyperfine interaction, to a nuclear spin $I = 1/2$, thereby reducing the number of resonance lines from three (for the $I = 1$ ^{14}N nitroxide) to two (Keith et al., 1974). This replacement increases the signal-to-noise ratio by an additional factor of 2 (Beth et al., 1981) and further enhances the angular resolution by reducing overlap between resonance lines that causes spin orientation ambiguities.

With [^{15}N,^2H]MTSL-S1, we decorate muscle fibers and measure their EPR spectra when the fibers are in rigor or in the presence of MgADP. The fiber symmetry axis is oriented either parallel or perpendicular to the Zeeman field. These experiments are similar to those done previously using MTSL-S1 (Ajtai et al., 1989). We find that the substituted probe shows an obvious spectral shape change from fibers oriented with fiber axis perpendicular to the Zeeman field when the cross-bridge binds nucleotide. This spectral change originates from a rotation of the spin probe about its torsional angle due to cross-bridge rotation.

Similar experiments were performed on 15IA-labeled muscle fibers. These data were combined with the EPR data from [^{15}N,^2H]MTSL-S1 and IPSL-S1 decorating muscle fibers to detect global angular transitions of the actin-bound myosin cross-bridge due to nucleotide binding, by the method described in the accompanying paper. We determine the angular distribution of each of the probes with resolution approaching the theoretical maximum. We find that probe sensitivity to cross-bridge rotation varies considerably from probe to probe. We also find that, if the shape of the cross-bridge is described as an ellipsoid with two equivalent minor axes, then cross-bridge rotation takes place mainly about an axis parallel to the major axis of the ellipsoid.

Theory

A. The Spin Hamiltonian. The appropriate spin Hamiltonian for the [^{15}N,^2H]MTSL, if we neglect the nuclear Zeeman interaction, is

$$\mathcal{H} = \beta_e \vec{H}\cdot\bar{\bar{g}}\cdot\vec{S} + g_e\beta_e\vec{I}\cdot\bar{\bar{T}}\cdot\vec{S} \quad (1)$$

where β_e is the Bohr magneton, $\vec{H}$ is the Zeeman field, $\bar{\bar{g}}$ is the g tensor, $\vec{S}$ is the electron spin of the nitroxide radical, g_e is the g factor of the free electron, $\vec{I}$ is the nuclear spin, and $\bar{\bar{T}}$ is the T sensor (Abragam & Bleany, 1970). Spin magnitudes $|\vec{I}|$ and $|\vec{S}|$ are both 1/2. We compute the matrix elements of the Hamiltonian from the basis set of spin states given by the products $|1/2,m_e\rangle|1/2,m_n\rangle = |m_e,m_n\rangle$, where subscript e (n) denotes the electronic (nuclear) spin wave function. This matrix is diagonalized, and the eigenvectors and eigenvalues are used in the calculation of the EPR spectrum by standard methods (Merzbacher, 1970).

The spin transition probability is

$$W_{i,j} = \langle i|\beta_e\vec{H}_1\cdot\bar{\bar{g}}\cdot\vec{S}|j\rangle \quad (2)$$

where $|i\rangle$ is an eigenvector of the Hamiltonian in eq 1 and $\vec{H}_1$ is the oscillating magnetic field that is perpendicular to the Zeeman field. There are six possible transitions, but $W_{i,j}$ is appreciable only for the transitions approximately corresponding to $m_n = +1/2$ and $-1/2$.

The EPR spectrum is sensitive to changes in the spin probe angular distribution involving any of three degrees of freedom corresponding to the Euler angles. The spectrum is least sensitive to changes in α since α dependence enters the line shape only through the transition probability $W_{i,j}$. We found by using simulations of EPR spectra that the α dependence of the line shape is negligible for the experimental conditions used here.

B. Probe Angular Distribution for Muscle Fibers. The probe angular distribution function N describes the orientation of a probe relative to a laboratory fixed reference frame. We expand N in terms of Wigner functions $\mathbf{D}^j_{m,n}$ that are complete on the interval $0 \le \alpha \le 2\pi$, $0 \le \beta \le \pi$, and $0 \le \gamma \le 2\pi$ such that

$$N(\Omega) = \sum_{j=0}^{\infty}\sum_{m,n=-j}^{j} a^j_{m,n}\sqrt{\frac{2j+1}{\beta\pi^2}}\,\mathbf{D}^j_{m,n}(\Omega) \quad (3)$$

where $\Omega = (\alpha,\beta,\gamma)$ are the Euler angles (Davydov, 1963). Euler angles α and β are the probe azimuth and polar angles relative to the fiber axis of symmetry, and γ is the torsion angle. The coefficients $a^j_{m,n}$ are the order parameters of rank j.

There is experimental evidence indicating that the fiber axis is a symmetry axis of the fiber (Burghardt et al., 1983). If the laboratory z-axis is assumed to be parallel to the fiber axis, then this symmetry implies that

$$a^j_{m,n} = a^j_{0,n}\,\delta_{m,0} \quad (4)$$

where $\delta_{i,j}$ is the Kronecker delta. A particular spin probe angular distribution is reconstructed from order parameters using eqs 3 and 4 such that

$$N(\beta,\gamma) = \sum_{j=0}^{j_{max}}\sum_{n=-j}^{j} a^j_{0,n}\sqrt{\frac{2j+1}{8\pi^2}}\,\mathbf{D}^j_{0,n} \quad (5)$$

The sum of j is terminated at j_{max}. The value of j_{max} depends on whether N is for a spin or fluorescent probe [see Burghardt and Ajtai (1992) under Theory, section D]. Two special cases derived from eq 5 that we use subsequently are the β-averaged distribution $m(\gamma)$, derived from $N(\beta,\gamma)$ by

$$m(\gamma) = \int_0^{\pi}(\sin\beta)N(\beta,\gamma)\,d\beta \quad (6)$$

and the γ-averaged distribution $n(\beta)$, derived from $N(\beta,\gamma)$ by

$$n(\beta) = \int_0^{2\pi}N(\beta,\gamma)\,d\gamma \quad (7)$$

C. Model Calculations. In some cases, a simple model of the spin probe angular distribution is useful to simulate changes in the EPR spectrum due to probe rotation. For this purpose, we use a Gaussian angular distribution of the form

$$N = N_0\exp\{-[(\cos\beta - \cos\beta_0)/w_1]^2 - [(\cos\gamma - \cos\gamma_0)/w_2]^2\} \quad (8)$$

where N_0 is a normalization constant determined by requiring that the sum of N over all possible orientations is unity, β_0 is the most probable polar angle the probe makes with the fiber axis, γ_0 is the most probable probe torsional angle, and the

w_i's are the distribution widths. This distribution is appropriate for a fiber with fiber axis parallel to the Zeeman field because N does not depend on α. The generalization of eq 8 to the probe distribution from fibers perpendicular to the Zeeman field is described in detail elsewhere (Burghardt & French, 1989).

Materials and Methods

Chemicals. The spin label [^{15}N,^{2}H]*N*-(1-oxyl-2,2,6,6-tetramethyl-4-piperidinyl)maleimide is a generous gift from Dr. Albert Beth, Department of Molecular Physiology and Biophysics, Vanderbilt University, Nashville, TN, 37232. The fluorescent label *N*-(iodoacetylaminoethyl)-5-naphthylamine-1-sulfonic acid was from Molecular Probes (Eugene, OR). ADP, ATP, P^1,P^5-di(adenosine 5')-pentaphosphate (Ap_5A), glucose, hexokinase, phosphocreatine, and creatine kinase are from Sigma (St. Louis, MO). Ammonium sulfate (ultra pure) is from Schwartz/Mann Biotechnology (Cleveland, OH). All chemicals are analytical grade.

Solutions. Rigor solution is 80 mM potassium chloride, 5 mM magnesium chloride, 2 mM ethylene glycol bis(β-aminoethyl ether)-*N*,*N*,*N'*,*N'*-tetraacetic acid (EGTA), and 5 mM phosphate buffer at pH 7.0. Relaxing solution is rigor solution with 4 mM ATP added. MgADP solution is rigor solution with 4 mM ADP, 100 μM Ap_5A to inhibit myofibrillar myokinase from converting ADP to ATP, and an ADP-regenerating system of 10 mM glucose and 0.1 mg/mL hexokinase to convert ATP to ADP. Activating solution is relaxing solution with 0.1 mM $CaCl_2$ replacing EGTA, 4 mM phosphocreatine, and 0.4 mg/mL creatine kinase to regenerate ATP. Rigor + glycerol solution is rigor solution in 50% glycerol (vol/vol; pH 7.0).

Preparation of Labeled Myosin Subfragment 1. Rabbit myosin was prepared by a standard method (Tonomura et al., 1966). We used α-chymotrypsin to digest myosin filaments in the preparation of myosin S1 (Weeds & Taylor, 1975).

The preparation of [^{15}N,^{2}H]MTSL-S1 in solution or precipitated in ammonium sulfate is identical to that of MTSL-S1 (Ajtai et al., 1990). The labeled protein is treated with potassium ferricyanide to selectively destroy radicals not linked to SH1 as described previously (Graceffa & Seidel, 1980; Ajtai et al., 1990). The specific labeling of SH1 on S1 with 15IA (15IA-S1) was carried out as described by Duke et al. (1976).

Specificity of Protein-Bound Spin Label. We measured the extent of spin labeling of the SH1's using K^+-EDTA and Ca^{2+} ATPase activities of labeled S1. Both ATPases of the [^{15}N,^{2}H]MTSL modified S1 behave in a manner identical to that of MTSL-modified S1 (Ajtai et al., 1990). The ATPase indicates specific and efficient (0.6–0.7 mol of spin label per mole of S1) modification of the SH1 group.

The EPR detection of protein-bound spin labels was carried out on [^{15}N,^{2}H]MTSL-S1 as described previously (Ajtai et al., 1990). Shown in Figure 1 are the EPR spectra from the SDS–PAGE isolated light chains (LC1 and LC2) and heavy chain of S1. The degree of specificity of the labeling of S1 is indicated by the intensity of the EPR spectrum measured from the isolated peptides. Identically to MTSL-S1, the dominant EPR signal (≥95%) from [^{15}N,^{2}H]MTSL-S1 originates from the heavy chain of S1. This result taken with the ATPase measurements again indicates specific labeling of SH1.

Muscle Fibers. We obtained rabbit psoas muscle fibers and decorated them with [^{15}N,^{2}H]MTSL-S1 as described previously (Ajtai et al., 1990).

We estimated the contribution of free [^{15}N,^{2}H]MTSL-S1 to the decorated fiber EPR spectrum by comparing the fiber

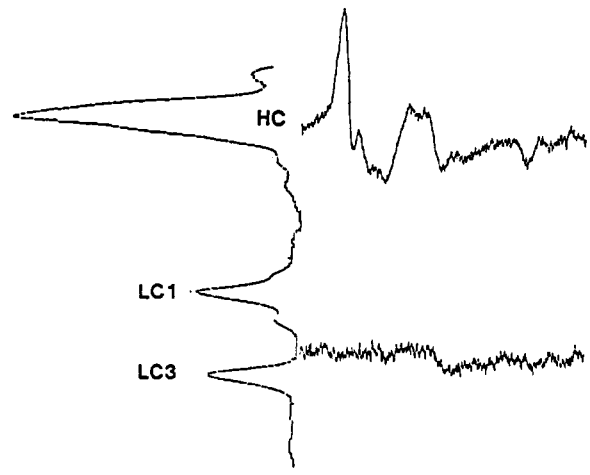

FIGURE 1: EPR spectrum of S1-bound spin label from SDS–PAGE electrophoretogram. The densitogram of a Coomassie-stained gel of [^{15}N,^{2}H]MTSL-S1 (left) indicates the presence of the myosin heavy chain (HC) and two light chains (LC1 and LC3). The EPR signal from gel bands containing these isolated peptides (right) shows the label is localized in the heavy chain. The EPR spectrum from the gel bands containing either LC1 or LC3 indicates only a background signal. Spectra were measured with a modulation amplitude of 1.0 G and a microwave power of 10 mW.

EPR spectrum to that obtained from [^{15}N,^{2}H]MTSL-S1 in solution. [^{15}N,^{2}H]MTSL-S1 in rigor or in the presence of MgADP had identical spectra that were characteristic of a randomly oriented slowly moving spin label. The spectrum from a decorated fiber with the fiber axis parallel to the Zeeman field shows a slight contribution from the low-field resonance characteristic of free [^{15}N,^{2}H]MTSL-S1. We estimated the contribution of free labeled protein to the decorated fiber spectrum to be ≤5%.

We prepared 15IA-labeled glycerinated muscle fibers using the procedure of Borejdo and Putnam (1977). The specificity of the probe for myosin SH1 in fibers was determined by several methods (Borejdo & Putnam, 1977; Ajtai & Burghardt, 1989). These data indicate that ~86% of the probe is localized on the myosin heavy chain with the other ~14% on actin and troponin I (Borejdo & Putnam, 1977). The myosin ATPases from myosin extracted from 15IA-labeled fibers indicate that all of the dye on the myosin heavy chain residues at SH1 (Ajtai & Burghardt, 1989). Modification of SH1 with 15IA does not impair fiber contractility even when the degree of labeling is as high as 0.8 mol of fluorophore per mole of myosin (Nihei et al., 1974).

Spectroscopic Measurements. All EPR measurements were carried out at room temperature using a TM_{110} cylindrical cavity as described previously (Ajtai et al., 1990).

The excitation polarization spectra of 15IA-S1 in solution and 15IA-labeled muscle fibers were measured as described previously (Ajtai & Burghardt, 1989). Fluorescence polarization studies on fibers were conducted at 4 °C. The solution studies were carried out on 15IA-S1 in rigor + glycerol solution at −15 °C to immobilize the probe–protein complex. The emission wavelength was selected with a cut-off filter that transmitted light of wavelengths ≥500 nm.

With the immobilized 15IA-S1, we measured the polarization anisotropy r, such that

$$r = \frac{f_{\parallel} - f_{\perp}}{f_{\parallel} + 2f_{\perp}} = (3\cos^2\theta - 1)/5 \qquad (9)$$

where f is the fluorescence intensity collected when the emission polarizer is oriented parallel ($\parallel$) or perpendicular ($\perp$) to the linear polarization of the excitation light. We measure

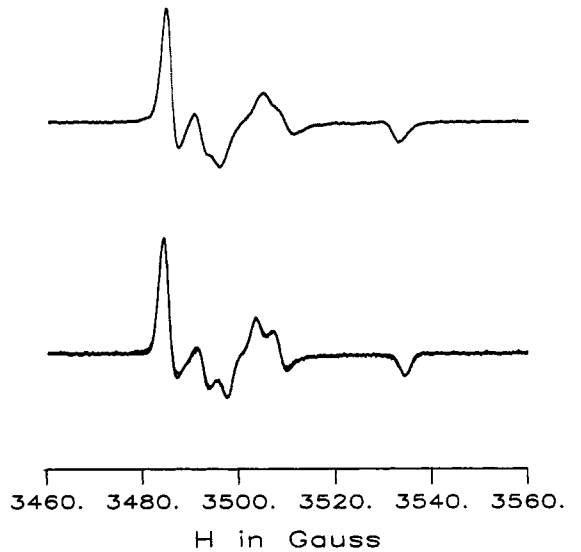

FIGURE 2: EPR spectra from [^{15}N,^{2}H]MTSL-S1 free in solution (top) and immobilized by precipitation in ammonium sulfate (bottom, dotted line). The spectrum from [^{15}N,^{2}H]MTSL-S1 free in solution is characteristic of a slowly moving randomly oriented spin probe. The spectrum from the immobilized probe is fitted (solid line) as described in the text (see Results, section A). Spectra were measured with a modulation amplitude of 0.5 G and a microwave power of 5 mW.

r to determine θ, the angle between the absorption and emission dipole of the fluorescent probe (Ehrenberg & Rigler, 1972). We summarize our data by plotting r and θ as a function of λ_{ex}, the excitation wavelength.

An experiment on labeled muscle fibers consists of measuring the polarization ratios $P_{\parallel}$, $P_{\perp}$, and $Q_{\parallel}$ defined in eqs 6–8 in the accompanying paper (Burghardt & Ajtai, 1992). We summarize our data by plotting $P_{\parallel}$, $P_{\perp}$, and $Q_{\parallel}$ as functions of λ_{ex}.

Results

A. EPR Spectrum of [^{15}N,^{2}H]MTSL-S1 in Solution and after Immobilization by Precipitation. The EPR spectrum of [^{15}N,^{2}H]MTSL-S1 in solution is shown in Figure 2 (top). This spectrum is identical to that from [^{15}N,^{2}H]MTSL-S1 in the presence of MgADP (data not shown) and indicates a slowly moving, randomly oriented probe and is very similar to that of [^{15}N,^{2}H]MTSL-labeled glyceraldehyde-3-phosphate dehydrogenase (GAPDHase) in solution (Beth et al., 1981). The EPR spectrum of [^{15}N,^{2}H]MTSL-S1 after precipitation with ammonium sulfate is shown in Figure 2 (bottom). This spectrum is best fitted using a random distribution of probes with a Gaussian line shape and the spectral parameters g_x = 2.0087 ± 0.0001, g_y = 2.0058 ± 0.0001, g_z = 2.0021 ± 0.0001, T_x = 10.7 ± 0.1 G, T_y = 10.7 ± 0.1 G, T_z = 49.7 ± 0.1 G, $h\nu/(\beta_e g_e)$ = 3509.3 G, where h is Planck's constant and ν is the microwave frequency, and a spectral line width of 1.3 ± 0.05 G. These values agree well with those obtained from immobilized [^{15}N,^{2}H]MTSL-GAPDHase (Beth et al., 1981).

The hyperfinc extrema from [^{15}N,^{2}H]MTSL-S1 in rigor or in the presence of MgADP, ΔH = 48.0 ± 0.2 G, is slightly smaller than that from immobilized [^{15}N,^{2}H]MTSL-S1, ΔH = 49.7 ± 0.1 G, indicating that the spin label is immobilized on the surface of S1 on the time scale of the spin relaxation and that the indicated slow rotational motion of [^{15}N,^{2}H]-MTSL-S1 in solution is from rotation of the probe–protein complex, in agreement with previous findings with MTSL-S1 (Ajtai et al., 1990).

B. EPR Spectrum of Oriented [^{15}N,^{2}H]MTSL-S1 Decorating Muscle Fibers. Figure 3 shows EPR spectra from

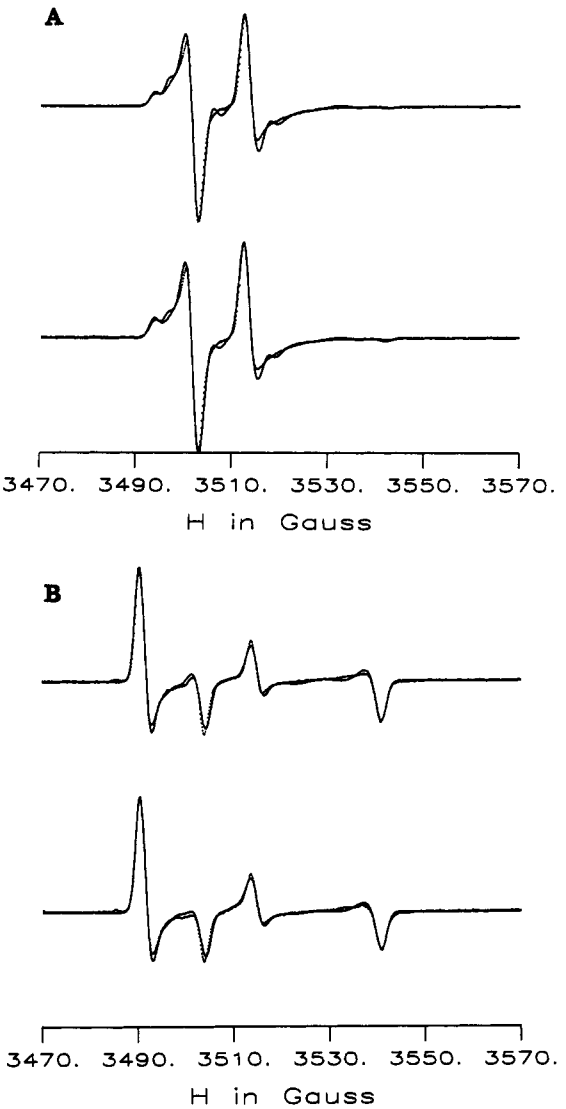

FIGURE 3: EPR spectra (dots) from muscle fibers decorated with [^{15}N,^{2}H]MTSL-S1 in rigor (top) and in the presence of MgADP (bottom), with fiber axis parallel (A) or perpendicular (B) to the Zeeman field. The spectra are fitted (solid line) as described in the text (see Results, section B). Spectra were measured with a modulation amplitude of 1.0 G and a microwave power of 10 mW.

[^{15}N,^{2}H]MTSL-S1 decorating muscle fibers for fibers oriented parallel (Figure 3A) or perpendicular (Figure 3B) to the Zeeman field in rigor (top) and in the presence of MgADP (bottom). We fitted 39 spectra simultaneously from 21 different fiber preprations using the order parameters determined by combining probe data sets from multiple probes of SH1, as described in the accompanying paper (Burghardt & Ajtai, 1992), and using the spectral parameter values obtained from precipitated [^{15}N,^{2}H]MTSL-S1 listed above.

The most apparent difference between the rigor vs MgADP spectra occurs in the perpendicular spectrum in the region 3485.0 G ≤ H ≤ 3500.0 G. Figure 4 shows this region of the perpendicular spectrum on an expanded scale for fibers in rigor (—) and in the presence of MgADP (- - -). Figure 5 shows simulated spectra from [^{15}N,^{2}H]MTSL-S1 for the model distribution of eq 8 with β_0 = 79.6°, w_1 = 15°, and γ_0 = 0°, w_2 = 5° (—·—) or γ_0 = 11°, w_2 = 10° (- - -) in the region 3480.0 G ≤ H ≤ 3500.0 G. This simulation qualitatively accounts for the change in the spectrum due to nucleotide binding as shown in Figure 4 and implies that the spectral change is due to a rotation of the cross-bridge that rotates the spin probe in its torsional (γ) degree of freedom.

FIGURE 4: Expanded scale view of Figure 3B showing the EPR spectra from muscle fibers perpendicular to the Zeeman field decorated with [^{15}N,^{2}H]MTSL-S1 in rigor (−·−) or in the presence of MgADP (-−-).

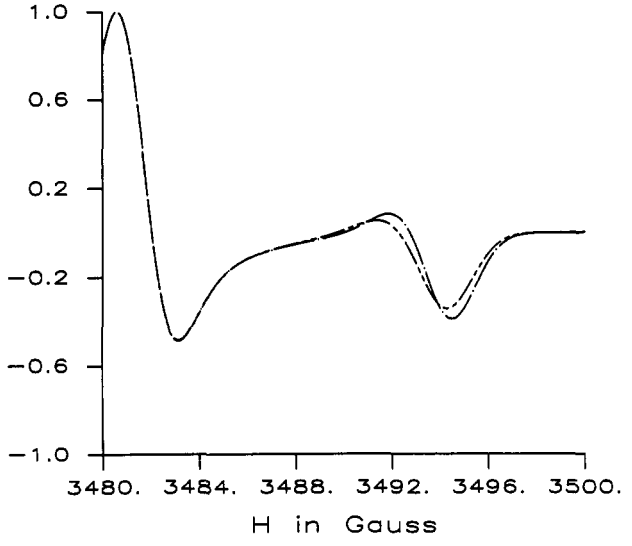

FIGURE 5: Simulated EPR spectra from the model probe angular distribution given by eq 8 for comparison with Figure 4. The spectral parameters and the model probe angular distribution parameters used in these simulations are given in the text (see Results, section B).

C. Fluorescence Polarization of Immobilized 15IA-S1 and 15IA-Labeled Muscle Fibers. Figure 6 shows the fluorescence polarization excitation spectrum of 15IA-S1 in 50% glycerol at −15 °C (random) and $P_{\parallel}$, $P_{\perp}$, and $Q_{\parallel}$ for fibers in rigor, in the presence of MgADP, in relaxation, and in contraction. The spectrum of 15IA-S1 in glycerol at −15 °C (randomly oriented and immobilized 15IA-S1) indicates the change in the relative orientation of the absorption and emission dipoles as a function of wavelength. The immobilized 15IA-S1 spectrum also defines the boundary that must be crossed to indicate the unambiguous detection of a probe rotation. Note, for instance, in Figure 6C where $Q_{\parallel}$ spectra from fibers in rigor and in the presence of MgADP fall below and above the random immobilized 15IA-S1 spectrum at and near to λ_{ex} = 360 nm. This region of the $Q_{\parallel}$ spectrum shows that the addition of random probe cannot alter the rigor spectrum to become the MgADP spectrum and consequently that probes in rigor must rotate to be distributed like probes in the presence of MgADP. Similar differences were observed between the active state and the three other physiological states of the muscle fiber studied, indicating that the contracting state has a unique orientation distribution that is distinguishable from

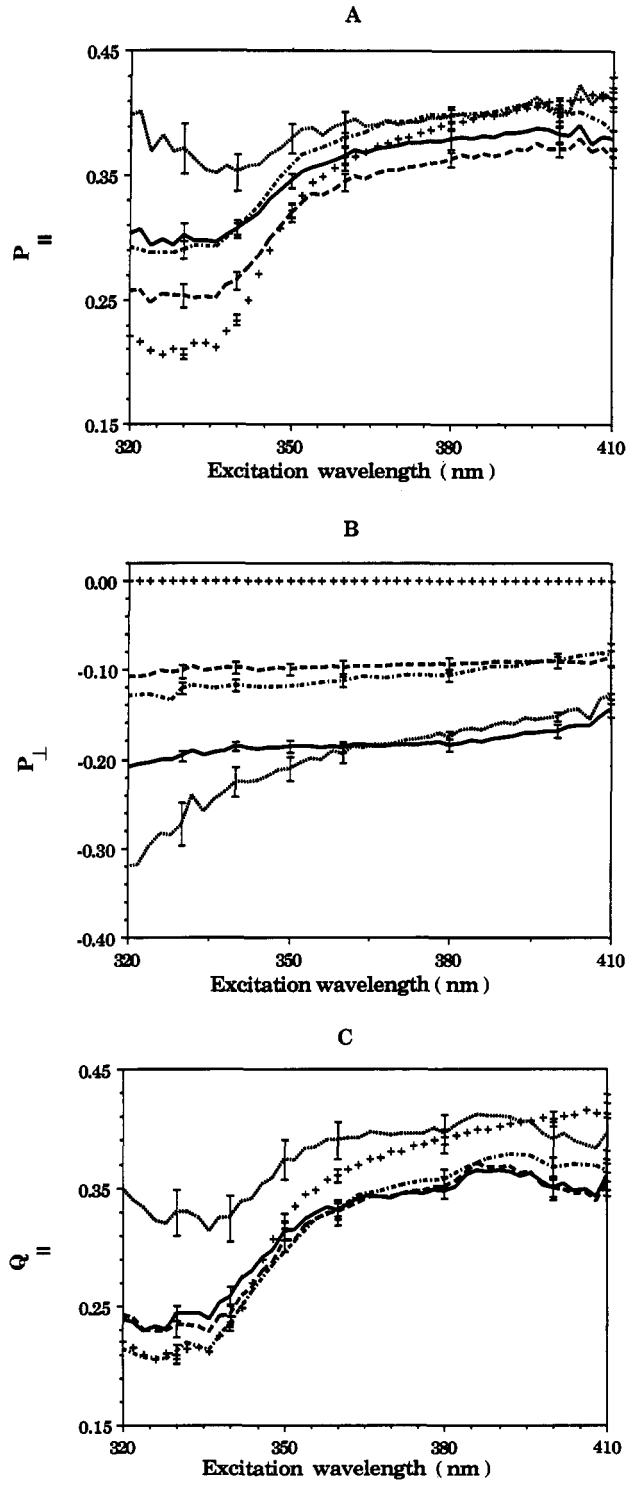

FIGURE 6: Fluorescence polarization excitation spectral ratios $P_{\parallel}$ (A), $P_{\perp}$ (B), and $Q_{\parallel}$ (C) from 15IA-labeled fibers in rigor (—), in the presence of MgADP (···), in relaxation (- - -), and contraction (-·-). $P_{\parallel}$ for randomly oriented and immobilized 15IA-S1 (+++) is also shown in each panel. Error bars represent standard error of the mean.

all of the other physiological states (see Figure 6, panels A–C).

Previous work with microscopic fluorescence polarization at fixed excitation wavelength, on 15IA-S1 decorating fibers in rigor and in the presence of MgADP, produced comparable results (Ajtai & Burghardt, 1987). The results differ from those presented here only in that two of the polarization ratios reflect somewhat higher order in the decorated system due to better probe specificity.

The polarization spectrum of random and immobilized 15IA-S1 is replotted as the anisotropy in Figure 7. Figure

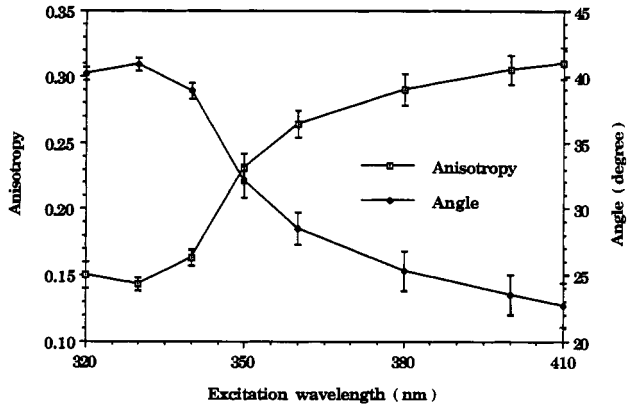

FIGURE 7: Fluorescence polarization excitation anisotropy and angle between the absorption and emission dipoles, θ, for 15IA-S1 in rigor with 50% glycerol at −15 °C. The anisotropy and the angle θ were computed from fluorescent intensities using eq 9. Error bars indicate standard deviation.

7 also contains a plot of θ, the angle between the absorption and omission dipoles computed from the anisotropy using eq 9. Over the domain of excitation wavelengths, 320 nm $\leq \lambda_{ex}$ 410 nm, θ ranges over ~20°.

D. Combining Probe Data Sets. The EPR spectra from [^{15}N,^{2}H]MTSL-S1 decorating muscle fibers and the polarization ratios $P_{\parallel}$, $P_{\perp}$, and $Q_{\parallel}$ at λ_{ex} = 330, 360, and 410 nm from 15IA-labeled fibers, the experimental data presented in this paper, are combined with the EPR spectra from IPSL-S1 decorating fibers measured previously (Ajtai et al., 1990) for fibers in rigor and in the presence of MgADP. These data supply the knowns in the system of equations developed for combining probe data sets as described in the accompanying paper (Burghardt & Ajtai, 1992). The solution to these equations consists of two parts: (i) the best choices for the Euler angles relating the individual probe molecular frames to each other and (ii) the best fitting set of probe order parameters. Below we report and discuss the values of these parameters in our best fitting solution.

D (i) Euler Angles. The Euler angles relating the probe molecular frames to each other, represented by Ω_i with i = 1, 2, ..., 5, and relating the laboratory frame to the molecular frame of IPSL-S1 in rigor fibers, represented by Ω_6, are summarized in Table I. The Euler angles Ω_i, i = 1, 2, ..., 5, are the best choices for satisfying the conditions on the Euler angles and probe order parameters summarized by eq 14 in the accompanying paper. No attempt was made to estimate the uncertainties in these angles since the computer time required to construct the 15-dimensional map of X^2 versus Euler angles is prohibitively large. The angles, Ω_6, relating the lab-fixed to a probe-fixed reference frame are plausible choices but do not necessarily reflect a quantitative result in the same sense as the other Euler angles (as discussed in section I under Theory in the accompanying paper.

The Euler angles Ω_i, i = 1, 2, ..., 5, are not uniquely determined since we showed that there are eight equivalent choices of these angles that satisfy the constraints of eq 14 in the accompanying paper. The equivalent sets of Euler angles, given in Table I of the accompanying paper each have a corresponding set of order parameters, but the equivalent Euler angles produce only four distinct sets of order parameters. These four sets of order parameters produce probe angular distributions, $N(\beta,\gamma)$, and three others produced by the substitutions $(\beta,\gamma) \rightarrow (\pi-\beta,\gamma)$, $(\beta,\pi+\gamma)$, or $(\pi-\beta,\pi+\gamma)$. Presently, these four solutions are equally likely to be the actual solution since we have no method to distinguish them. The ambiguities, reflected by these equivalent solutions, do not alter our subsequent conclusions concerning the myosin cross-bridge rotation.

Table I: Euler Angles Relating Probes of Myosin SH1[a]

α_1 = 85	β_1 = 30	γ_1 = 65	ϕ_1 = 151
α_2 = 86	β_2 = 11	γ_2 = 274	ϕ_2 = 11
α_3 = 42	β_3 = 27	γ_3 = 54	ϕ_3 = 99
α_4 = 63	β_4 = 34	γ_4 = 32	ϕ_4 = 100
α_5 = 68	β_5 = 40	γ_5 = 28	ϕ_5 = 102
α_6 = 273	β_6 = 69	γ_6 = 151	ϕ_6 = 91

[a] Euler angles given in degrees relating the probe fixed reference frames of [^{15}N,^{2}H]MTSL with IPSL ($\alpha_1,\beta_1,\gamma_1$), cross-bridges in rigor with cross-bridges in the presence of MgADP ($\alpha_2,\beta_2,\gamma_2$), IPSL with 15IA at λ_{ex} = 330 nm ($\alpha_3,\beta_3,\gamma_3$), IPSL with 15IA at λ_{ex} = 360 nm ($\alpha_4,\beta_4,\gamma_4$), IPSL with 15IA at λ_{ex} = 410 nm ($\alpha_5,\beta_5,\gamma_5$), and the laboratory fixed frame with IPSL in rigor ($\alpha_6,\beta_6,\gamma_6$). Angles ϕ_i, i = 1, 2, ..., 6, represent the magnitude of the principal axis rotation equivalent to the Euler rotation ($\alpha_i,\beta_i,\gamma_i$).

Any Euler rotation of coordinates can be represented by a rotation through angle ϕ, about a single principal axis (Arfken, 1970). Also summarized in Table I are the ϕ's for the six Euler rotations. Of particular interest is ϕ_2, indicating the magnitude of the principal axis rotation required to make the rigor-to-MgADP state transition. The value of ϕ_2 represents an upper limit on the orientation change that could be detected by direct experimental measurement and is in rough agreement with that estimated by measurement of the orientation changes of (iodoacetamido)tetramethylrhodamine (IATR) labeling SH1 in muscle fibers in rigor when the cross-bridge binds MgADP (Burghardt et al., 1983). Data from IATR-labeled and IATR-S1-decorated fibers suggested that the cross-bridges rotate ~10° and ~20°, respectively, from their orientation in rigor upon binding MgADP. This comparison implies that our present solution involving two spin labels and 15IA are consistent with the results from IATR if the cross-bridge is a rigid body.

In our description of the probe distribution relative to the laboratory frame, we choose to lab z-axis parallel to the fiber axis, the fluorescent probe z-axis parallel to the probe absorption dipole and the xz-plane to contain the emission dipole, and the spin probe reference frame equal to the principal magnetic frame. For both EPR and fluorescence polarization, the magnitude of the projection of the probe fixed z-axis onto the lab z-axis is the most sensitively detected parameter varying with probe orientation and is proportional to cos β. The orientation of the probe xz-plane is related to the torsion angle γ and is less sensitively detected by our techniques.

We attempted to qualitatively investigate the rotation of the probe fixed reference frame by estimating the most probable orientation of this frame for the various conditions investigated experimentally. We estimated these orientations by rotating the lab frame to the probe frame of IPSL-S1 decorating muscle fibers in rigor using the Euler angles Ω_6 and then rotating subsequently to every other possible probe frame using the Euler angles Ω_i, i = 1, 2, ..., 5. We chose the best values for Ω_6 by maximizing the sum of the overlaps from each probe distribution. This procedure was described in more detail in section I under Theory in the accompanying paper.

Figure 8 shows the stereodrawings of the three-dimensional position of the molecule fixed reference frame for the spin and fluorescent probes. The figure is drawn with uncrossed visual axes for viewing with a stereoscope. Figure 8, panels A–D, shows the rigor-to-MgADP rotational transition and the principal axis of rotation of this transition for [^{15}N,^{2}H]MTSL, IPSL, and 15IA at λ_{ex} = 330 and 410 nm. In each case, the rigor-to-MgADP transition is an 11° rotation about the principal axis.

The spin labels are viewed from identical perspectives relative to the laboratory frame. The molecule fixed reference frame of [^{15}N,^{2}H]MTSL-S1 in Figure 8A indicates that the rigor-to-MgADP transition is a general rotation that causes a reorientation of all of the axes in the molecular frame. The projection of the [^{15}N,^{2}H]MTSL z-axis onto the lab z-axis changes only slightly, accounting for approximately a 2° change in the polar angle of the probe. The torsional angular change is larger at ~7°. The molecule fixed reference frame of IPSL-S1 in Figure 8B indicates that the rigor-to-MgADP transition is a polar angle rotation of the probe of ~6° and the torsional angular change is ~3°.

The fluorescent probe molecular frame rigor-to-MgADP transitions shown in Figure 8, panels C and D, follow a similar pattern to the spin labels. Figure 8 panels C and D have identical perspectives relative to the lab frame and differ only in the excitation light wavelength, λ_{ex}, as indicated. For λ_{ex} = 330 nm, the projection of the absorption dipole (the probe z-axis) onto the lab z-axis changes during the rigor-to-MgADP transition such that the dipole polar angle changes ~5°. In this case, the torsional angular change is ~4°. For λ_{ex} = 410 nm, the absorption dipole polar angle changes by ~2° while the torsional angular change is ~10°.

The Euler angles connecting the molecular frames of the 15IA probe at λ_{ex} = 330, 360, and 410 nm give the angular trajectory of the absorption and emission dipoles as a function of wavelength. In this application, emission wavelength was not varied so we expect that the emission dipole is unchanged while the absorption dipole rotates through an angular path determined by the Euler angles of Table I. Shown in Figure 8E are the absorption and emission dipoles of 15IA-labeled muscle fibers in rigor as a function of wavelength. The emission dipole $\vec{\mu}_e$ is unchanged by excitation wavelength variation and the absorption dipole $\vec{\mu}_a$ varies as shown for 330 nm $\leq \lambda_{ex} \leq$ 410 nm. The molecular frame y-axis is perpendicular to both $\vec{\mu}_e$ and $\vec{\mu}_a$.

We will show subsequently that these qualitative findings summarized in Figure 8 are confirmed by the more rigorous probe angular distributions computed from order parameters. We discuss the probe angular distributions below.

D (ii) Probe Angular Distributions. The probe angular distributions are computed from the order parameters as described under Theory in this paper. For all of the probes, order parameters of rank j = 0, 2, 4, and 6 are used in these computations. Some of the higher rank order parameters are also determined for the spin probes, and these parameters are used in the computation of the spin probe angular distributions.

D (iia) [^{15}N,^{2}H]MTSL-S1 Decorating Muscle Fibers. Figure 9A shows the angular distribution of [^{15}N,^{2}H]-MTSL-S1 decorating muscle fibers in rigor and in the presence of MgADP. The β-averaged distribution, $m(\gamma)$, is computed using eq 6 (Figure 9A, left). Because of the residual ambiguity in our method of determining the probe angular distribution, $m(\gamma)$ is invariant under the transformation $\gamma \rightarrow \gamma+\pi$. The shapes of the distributions are similar for the two fiber states, but the major component of the spin density in both distributions (oriented near to γ = 0°) represents ~10% more of the total spin density when the fiber is in rigor compared to that in the presence of nucleotide. This plot does not indicate a new well-defined orientation that is populated when the cross-bridge binds MgADP although the position of the main peak shifts ~4° in this case.

Figure 9A also shows the γ-averaged distribution $n(\beta)$, computed using eq 7. Because of the residual ambiguity in our method of determining the probe angular distribution, $n(\beta)$ is invariant under the transformation $\beta \rightarrow \pi-\beta$ (Figure 9A, right). Again the shape of the distributions are similar for the two fiber states, but the distribution maxima near to β = 90° represent ~5% more of the total density when the fiber is in rigor compared to that in the presence of MgADP. Clearly, a significant amount of spin density shifts from the main peak to a secondary peak near to β = 0 when the cross-bridge binds MgADP.

D (iib) IPSL-S1 Decorating Muscle Fibers. Figure 9B shows the angular distribution of IPSL-S1 decorating muscle fibers in rigor and in the presence of MgADP. This spin probe labels the cross-bridge at SH1 but is oriented differently than [^{15}N,^{2}H]MTSL in the cross-bridge molecular frame. In contrast to [^{15}N,^{2}H]MTSL-S1, $m(\gamma)$ indicates no significant change in the spin density from rigor fibers when MgADP binds to the cross-bridge (Figure 9B, left). Nevertheless, $n(\beta)$ shows a large shift in the distribution of rigor cross-bridges such that ~10% of the probe density rotates from the peak at β = 90° to a secondary peak nearer to β = 0 when the cross-bridge binds MgADP (Figure 9B, right). The primary peak at β = 90° corresponds to ~60% or ~50%, and the secondary peak to ~40% or ~50%, of the total spin density in rigor or in the presence of MgADP. The $n(\beta)$ plot presented here differs qualitatively with the previous determination of $n(\beta)$ based on the direct analysis of EPR spectra from IPSL-S1 decorating fibers in rigor and in the presence of MgADP (Ajtai et al., 1990). These differences reflect enhancements due to the global nature of the present solution that combines the input from multiple probes of the myosin cross-bridge.

These two spin labels of S1 indicate the same phenomena of actin-bound cross-bridge rotation when the cross-bridge binds nucleotide but through different angular degrees of freedom. Since the spin labels detect changes in the polar angle β, more readily than changes in the torsional angle γ, the IPSL probe is more suitable for detection of cross-bridge rotation in fibers.

D (iic) 15IA-Labeled Muscle Fibers. Figure 10A shows the angular distribution of the absorption dipole of 15IA-labeled muscle fibers in rigor and in the prescence of MgADP for the excitation wavelength of 330 nm. The $m(\gamma)$ and $n(\beta)$ distributions show modest differences between rigor and the MgADP states. The $n(\beta)$ distribution (Figure 10A, right) indicates cross-bridge rotation in the β degree of freedom somewhat more strongly than the $m(\gamma)$ distribution (Figure 10A, left).

Figure 10B shows the equivalent angular distributions for 15IA-labeled fibers when the excitation wavelength is 410 nm. At this wavelength, $m(\gamma)$ shows a larger contrast between the two states of the fiber than $n(\beta)$ (compare Figure 10B, left with Figure 10B, right). The comparison of the angular distributions of 15IA at the two excitation wavelengths shows the differential sensitivity of the probe to cross-bridge rotation due to the orientation of the absorption dipole in the cross-bridge molecular frame (compare Figure 10 panels A and B). Equivalent plots of the angular distribution of 15IA-labeled fibers when the excitation wavelength is 360 nm indicate results intermediate between those for 330- and 410-nm excitation.

Discussion

We used a sensitive spin probe to detect myosin cross-bridge orientation changes in muscle fibers. The importance of this probe is that it allowed us to detect an obvious spectral change and thereby to confirm a previous observation concerning cross-bridge orientation differences from fibers in rigor compared to that in the presence of MgADP. Previously, we

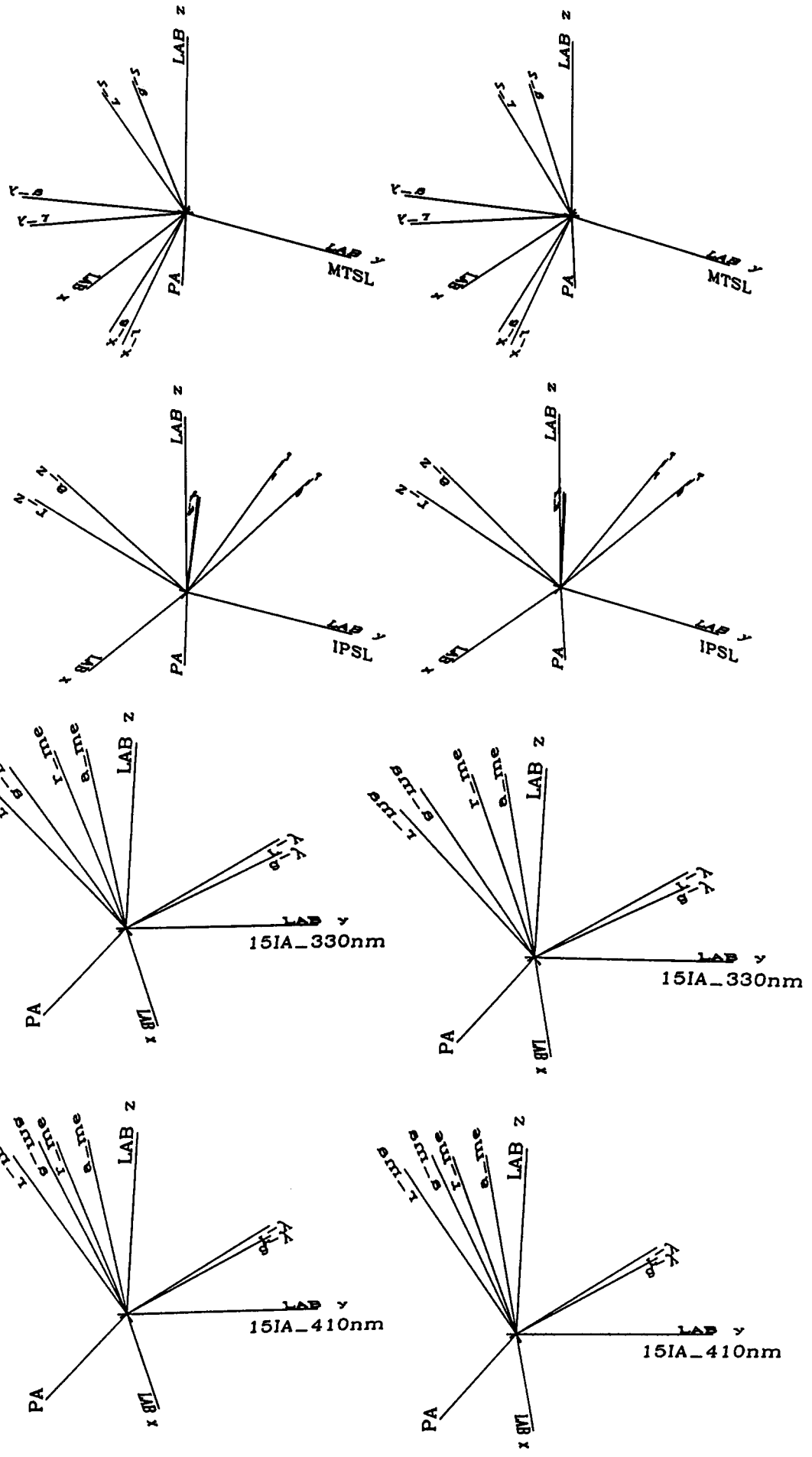
LAB z
LAB y
PA
MTSL
IPSL
15IA_330nm
15IA_410nm

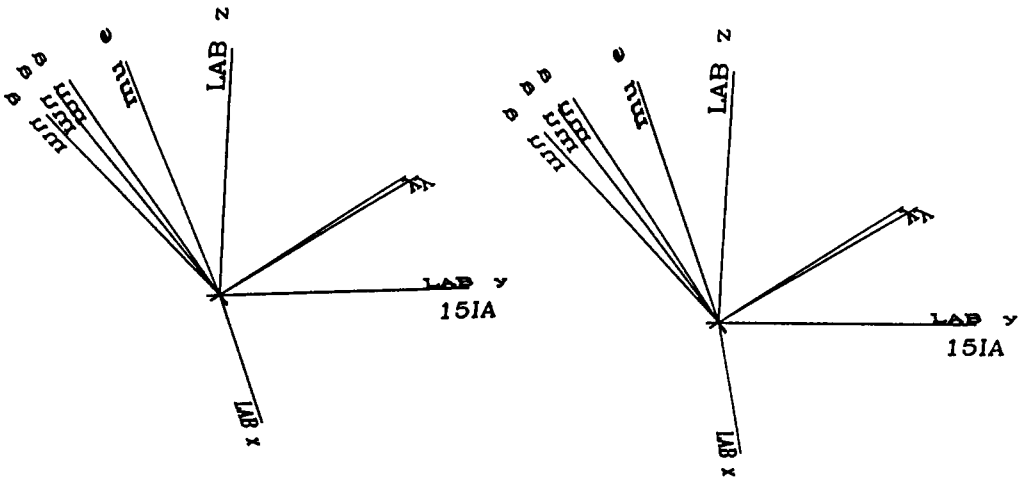

FIGURE 8: Uncrossed stereodrawings of the laboratory fixed reference frame and the probe fixed frame for [^{15}N,^{2}H]MTSL-S1 (A, opposite page, top) and IPSL-S1 (B, opposite page, second from top) decorating muscle fibers, and 15IA-labeled fibers at λ_{ex} = 330 nm (C, opposite page, second from bottom) and 410 nm (D, opposite page, bottom), for fibers in rigor (r) and in the presence of MgADP (a). Also shown in each panel is the principal axis (PA) of rotation of the rigor-to-MgADP transition. Panel E (this page, above) indicates the angular trajectory of the absorption dipole ($\vec{\mu}_a$) as a function of excitation wavelength for the points λ_{ex} = 330, 360, and 410 nm. The emission dipole ($\vec{\mu}_e$) remains the same for each excitation wavelength. The angle between $\vec{\mu}_a$ and $\vec{\mu}_e$ is largest for λ_{ex} = 330 nm and smallest for λ_{ex} = 410 nm.

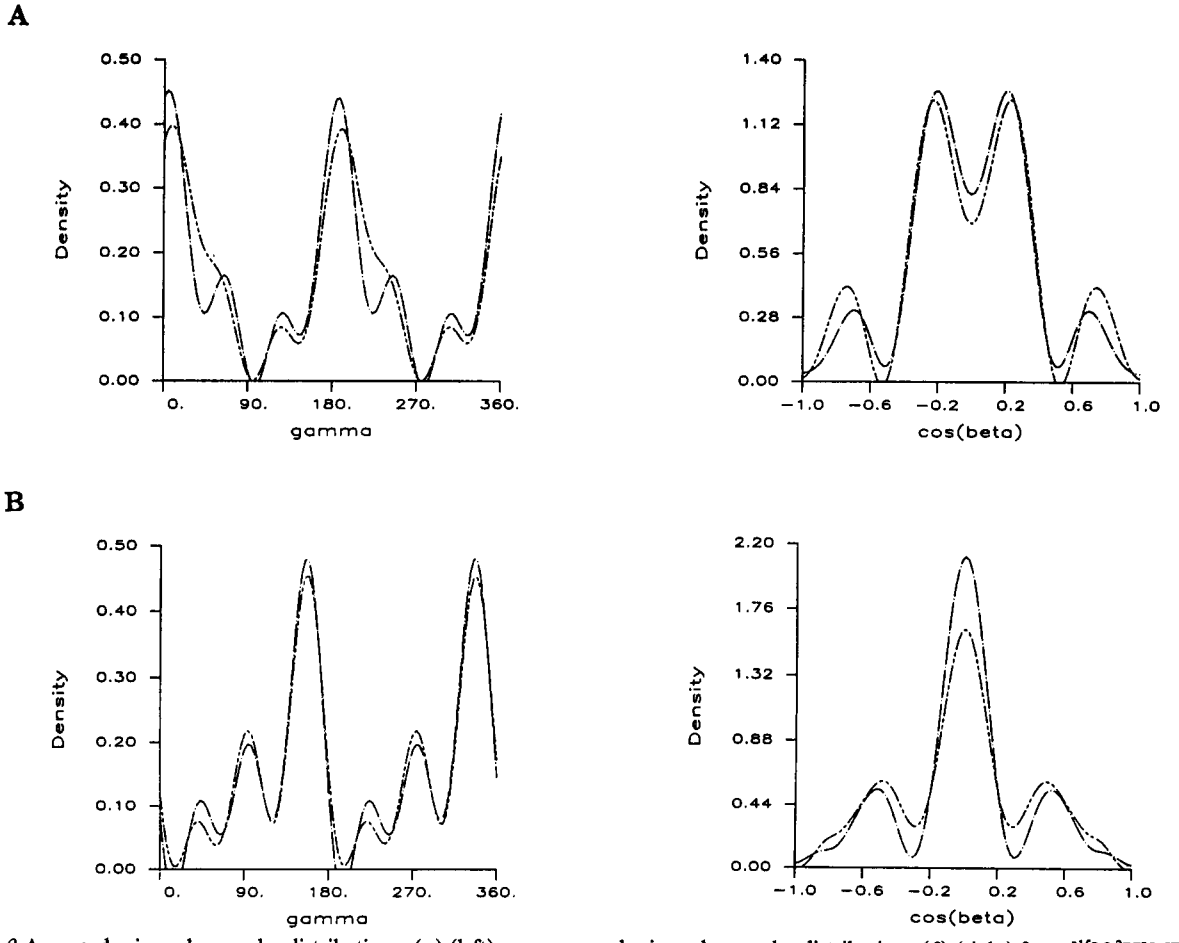

FIGURE 9: β-Averaged spin probe angular distribution $m(\gamma)$ (left) or γ-averaged spin probe angular distribution $n(\beta)$ (right) from [^{15}N,^{2}H]MTSL-S1 (panel A) or IPSL-S1 (panel B) decorating muscle fibers in rigor (–·–) and in the presence of MgADP (- - -). The plots indicate the changes in the torsional (left) or polar (right) degree of freedom of the spin probe when the cross-bridge binds MgADP.

studied muscle fibers decorated with MTSL-S1 and concluded that the cross-bridge rotates upon binding MgADP in a manner that rotates the spin probe in its torsion angle (Ajtai et al., 1989). This conclusion is not evident from the EPR spectra measured from the decorated muscle fibers but was deduced from a detailed model-independent study of the spectral shape. The ^{15}N- and ^{2}H-substituted maleimido-TEMPO probe greatly enhances the angular resolving power of the EPR spectrum. We reinvestigated the rotation of actin-bound myosin cross-bridges that occurs when the cross-bridges also bind MgADP using [^{15}N,^{2}H]MTSL-S1 decorating muscle fibers. We wanted to see if the substituted probe could more readily detect this rotation. The data presented here definitively confirm our earlier conclusion and demonstrate that EPR spectra from [^{15}N,^{2}H]MTSL-S1 decorated fibers perpendicular to the Zeeman field show an evident change,

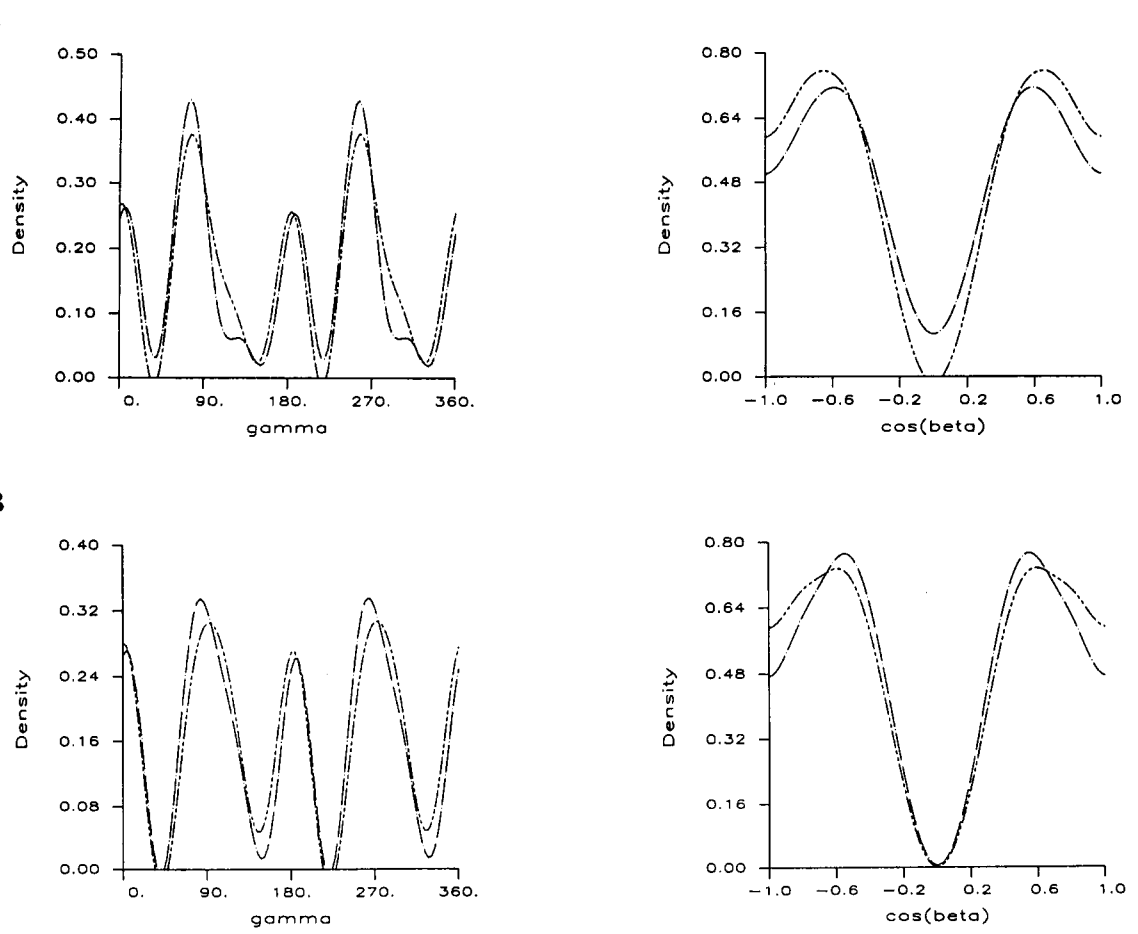

FIGURE 10: β-Averaged fluorescent probe angular distribution $m(\gamma)$ (left) or γ-averaged fluorescent probe angular distribution $n(\beta)$ (right) from 15IA-labeled fibers, excited with light of wavelength 330 nm (panel A) or 410 nm (panel B), in rigor (—·—) and in the presence of MgADP (- - -). The plots indicate the changes in the torsional (left) or polar (right) degree of freedom of the fluorescent probe when the cross-bridge binds MgADP.

due to the nucleotide binding to the cross-bridge, that can be directly attributed to a change in the torsion angle of the probe.

We also applied the analytical method described in the accompanying paper (Burghardt & Ajtai, 1992) to combine data from multiple probes of myosin SH1 to enhance the angular resolution of the individual probe distributions with the purpose of mapping global angular transitions of the myosin cross-bridge. The results of this analysis are summarized in Figures 9 and 10 where we demonstrate the differential sensitivity of the extrinsic probes to cross-bridge rotation. [^{15}N,^{2}H]MTSL-S1 decorating muscle fibers and 15IA-labeled fibers excited at λ_{ex} = 410 nm detect cross-bridge rotation as a change in the torsional degree of freedom of the probe. This degree of freedom is the least detectable parameter such that large changes in it produce only slight changes in the observed signal. IPSL-S1 decorating muscle fibers and 15IA-labeled fibers excited at $\lambda_{ex} \leq 360$ nm detect cross-bridge rotation as a change in the polar degree of freedom of the probe. The observed signal changes significantly with only a slight change in this degree of freedom.

The Euler angles connecting the individual probe molecular frames also indicate the means by which the probes detect cross-bridge rotation. For instance, comparison of panels A and B in Figure 8 indicates the two possibilities for detecting cross-bridge rotation for spin probes, i.e., as a rotation in its torsional degree of freedom as for [^{15}N,^{2}H]MTSL-S1 (Figure 8A) or as a rotation in its polar angular degree of freedom as for IPSl-S1 (Figure 8B). In the case of the fluorescent probe, the above applies (see Figure 8, panels C and D) and in addition the Euler angles indicate the angular trajectory of the absorption dipole as a function of excitation wavelength. Points on the three-dimensional trajectory are plotted in Figure 8E. We have noted that the ability to rotate the transition dipole experimentally was essential to confirming the observation of cross-bridge rotation. Visualizing the orientation of the dipoles in space during the rotational transition of the cross-bridge helps to suggest a possible mechanism of cross-bridge rotation as discussed below.

Independent direction-reporting probes, with various orientations relative to the cross-bridge molecular frame, were used to reduce or eliminate ambiguities in the detection of cross-bridge rotation (Ajtai & Burghardt, 1989). The combination of data sets from different probes and different techniques to amplify the resolution of each probes angular distribution, by the method described here, was not done previously. With this method we extend the angular resolution of both fluorescent and spin probes to an extent that approaches the theoretical limit.

The enhanced resolution probe angular distributions, produced by our method of combining multiple probe data sets, suggest that the cross-bridge can bind to the actin filament with more than one distinct orientation and that the observed probe distribution is a weighted sum over the distinct cross-bridge orientations. The relative weight of each orientation is determined by the physiological state of the fiber. This idea is supported by all of the angular distributions but is most clearly indicated by the γ-averaged spin probe distributions, $n(\beta)$, of Figure 9 (right). The occupancy of the spin popu-

lations is modulated by nucleotide binding to the cross-bridge.

The orientation of 15IA relative to the hydrodynamic reference frame of S1 was estimated from 15IA-S1 tumbling in solution using time-resolved fluorescence anisotropy decay (TRFAD) with 330 nm $\leq \lambda_{ex} \leq$ 380 nm (Mendelson et al., 1973). In this work, it was assumed that S1 is an ellipsoid with two equivalent minor axes. Under this assumption, the z-axis of the principal hydrodynamic reference frame is parallel to the major axis of the ellipsoid. The TRFAD measurements indicated that the absorption and emission dipoles of the 15IA made an angle of $\leq 40°$ with the z-axis of the principal hydrodynamic frame so that the angular distribution of the 15IA probe modifying SH1 approximately reflects the distribution of the principal hydrodynamic frame of S1. From the work presented here, we found that, at each of the excitation wavelengths tried, the rigor-to-MgADP transition in the actin-bound cross-bridge caused a rotation of the 15IA in its torsional degree of freedom and therefore that the hydrodynamic frame of S1 is similarly rotating in its torsional degree of freedom. We speculate that the rigor-to-MgADP cross-bridge state transition may indicate the motion of cross-bridges during muscle concentration (in this case the power stroke would be modeled as the reverse of the rigor-to-MgADP state transition) and suggest future experimental investigation of cross-bridge rotation include the possibility of torsional motion.

ACKNOWLEDGMENTS

We thank Dr. Albert Beth of the Department of Molecular Physiology and Biophysics, Vanderbilt University, Nashville, TN, for the gift of the [^{15}N,^{2}H]MTSL and Dr. Franklyn Prendergast of the Mayo Foundation for helpful discussions.

Registry No. MgADP, 7384-99-8; [^{15}N,^{2}H]MTSL, 137564-76-2; *N*-(iodoacetylaminoethyl)-5-naphthylamine-1-sulfonic acid, 36930-63-9.

REFERENCES

Abragam, A., & Bleany, B. (1970) *Electron Paramegnetic Resonance of Transition Ions*, pp 133–209, Dover, NY.

Ajtai, K., & Burghardt, T. P. (1987) *Biochemistry 26*, 4517–4523.

Ajtai, K., & Burghardt, T. P. (1989) *Biochemistry 28*, 2204–2210.

Ajtai, K., French, A. R., & Burghardt, T. P. (1989) *Biophys. J. 56*, 535–541.

Ajtai, K., Pőtő, L., & Burghardt, T. P. (1990) *Biochemistry 29*, 7733–7741.

Arfken, G. (1970) *Mathematical Methods for Physicists*, pp 195, Academic Press, NY.

Beth, A. H., Venkataramu, S. D., Balasubramanian, K., Dalton, L. R., Robinson, B. H., Pearson, D. E., Park, C. R., & Park, J. H. (1981) *Proc. Natl. Acad. Sci. U.S.A. 78*, 967–971.

Borejdo, J., & Putnam, S. (1977) *Biochim. Biophys. Acta 459*, 578–595.

Burghardt, T. P., & Thompson, N. L. (1985) *Biophys. J. 48*, 401–409.

Burghardt, T. P., & French, A. R. (1989) *Biophys. J. 56*, 525–534.

Burghardt, T. P., & Ajtai, K. (1992) *Biochemistry* (preceding paper in this issue).

Burghardt, T. P., Ando, T., & Borejdo, J. (1983) *Proc. Natl. Acad. Sci. U.S.A. 80*, 7515–7519.

Davydov, A. S. (1963) *Quantum Mechanics*, pp 145–169, NEO Press, Ann Arbor, MI.

Duke, J., Takashi, R., Ue, K., & Morales, M. F. (1976) *Proc. Natl. Acad. Sci. U.S.A. 73*, 302–306.

Ehrenberg, M., & Rigler, R. (1972) *Chem. Phys. Lett. 14*, 539–544.

Graceffa, P., & Seidel, J. C. (1980) *Biochemistry 19*, 33–39.

Keith, A., Horvath, D., & Snipes, W. (1974) *Chem. Phys. Lipids 13*, 49–62.

Huang, J. S., Mason, R. P., Hwang, L. P., & Freed, J. H. (1975) *J. Phys. Chem. 79*, 489–511.

Mendelson, R. A., Morales, M. F., & Botts, J. (1973) *Biochemistry 12*, 2250–2255.

Merzbacher, E. (1970) *Quantum Mechanics*, pp 413–450, John Wiley, New York.

Nihei, T., Mendelson, R. A., & Botts, J. (1974) *Biophys. J. 14*, 236–242.

Tonomura, Y., Appel, P., & Morales, M. F. (1966) *Biochemistry 5*, 515–521.

Weeds, A. G., & Taylor, R. S. (1975) *Nature (London) 257*, 54–56.